IDŐJÁRÁS

Quarterly Journal of the Hungarian Meteorological Service
Vol. 119, No. 1, January – March, 2015, pp. 1–21

Expected changes in mean seasonal precipitation and temperature across the Iberian Peninsula for the 21st century

Joan Ramon Coll[1], **Philip D. Jones**[2, 3], and **Enric Aguilar**[1]

[1] *Centre for Climate Change, Geography Department, Rovira i Virgili University, Av. Remolins 13-15, 43500 Tortosa, Spain.*

[2] *Climatic Research Unit, School of Environmental Sciences, University of East Anglia, Norwich, NR4 7TJ, UK.*

[3]*Center of Excellence for Climate Change Research, Department of Meteorology, King Abdulaziz University, Jeddah 21589, Saudi Arabia*

**Corresponding author E-mail: joanramon.coll@urv.cat*

(Manuscript received in final form April 24, 2014)

Abstract—Three different regional climate models (DMI-HIRHAM5, HadRM3, and KNMI-RACMO2) driven by ERA-40 reanalysis and also driven by global climate models (GCMs) obtained from the EU-Ensembles project have been compared to observed data over the Iberian Peninsula (IP) to assess the accuracy of simulated precipitation and temperature. KNMI-RACMO2 and DMI-HIRHAM5 were the best models for accurately simulating precipitation and temperature, respectively, although large uncertainties still affect their simulations. The same RCM simulations driven by GCMs have been used to project the seasonal expected changes in precipitation and temperature for the periods 2011–2050 and 2051–2090 relative to 1961–2000 under the A1B climate change scenario. From the results, a clear decrease in mean precipitation is expected in most IP for spring, summer, and autumn, but no clear signal was found in winter. Moreover, future projections showed a large increase in mean temperatures in all seasons being more evident in the interior of the IP especially in summer. The decrease in mean precipitation and the increase in mean temperature projected for the IP, could worsen current drought conditions especially for the second half of the 21st century.

Key-words: regional climate models, Iberian Peninsula, precipitation, temperature, model accuracy validation, future projections, drought

1. Introduction

Future climate will include simultaneous changes in temperature and precipitation for many regions of the world. For example, in the Iberian Peninsula (IP), the observed and projected increase in temperature is expected to be accompanied by a decrease in precipitation (*IPCC,* 2007; *Sousa et al.,* 2011; *IPCC,* 2012). This combination would have a negative impact on water availability.

Previous studies have confirmed a warming trend in the 20th century across the IP using observed data (*Brunet et al.,* 2006; *Brunet et al.,* 2007), while precipitation patterns showed a high inter-annual variability, but appreciable changes have not still been identified in annual precipitation totals (*Barrera-Escoda,* 2008; *CLIVAR*, 2010).

Being consistent with the observed trends, climate models project a large increase in temperatures, but also a future decrease in precipitation of roughly 20% in southern Europe by the end of 21st century (*IPCC,* 2007) including the whole IP (*Sánchez*, 2009; *Gómez-Navarro et al.,* 2010; *Rodríguez-Puebla* and *Nieto,* 2010; *Vicente-Serrano et al.,* 2011; *Jerez et al.,* 2012; *Jerez* and *Montavez*, 2012). Again, this warming/drying combination implies an increase of drought conditions over the wider Mediterranean region (*Blenkinsop* and *Fowler,* 2007; *Mariotti et al.,* 2008; *Dai,* 2011 and 2012; *IPCC,* 2012) and also over the IP (*Beniston et al.,* 2007; *Rodríguez-Puebla* and *Nieto,* 2010;; *Sanchez et al.,* 2012). These consistent results, obtained through the analysis of model output, have to be put in the context of the large uncertainties related to the reliability of model simulations affecting the projections of trends in temperature, precipitation, and drought conditions for the coming century (*Blenkinsop* and *Fowler,* 2007; *Sheffield* and *Wood*, 2008; *Rammukainen,* 2010; *Mishra* and *Singh*, 2011; *IPCC,* 2012; *Dai*, 2012).

This article focuses on investigating the capability of three regional climate models to correctly reproduce future temperature and precipitation in the IP. We used the outputs from the RCMs driven by ERA-40 reanalysis for the period 1958–2002 to make comparisons with observed data and the same RCMs driven by associated GCMs for future projections covering the period 1951–2100. We approach this analysis by comparing climate model output belonging to the A1B climate change scenario to an overlapping observational dataset of temperature and precipitation.

2. Data

Monthly simulated temperature and precipitation data from three regional climate models (RCMs) at 25 km resolution were obtained from the EU-Ensembles project (available at http://www.ensembles-eu.org). DMI-HIRHAM5 produced by the Danish Meteorological Institute (DMI) (*Christensen* and

Christensen, 2007), HadRM3 using the HC-Q0 (normal sensitivity) developed by the Hadley Centre for Climate Prediction and Research (HC) (*Collins et al.*, 2010), and KNMI-RACMO2 produced by the Royal Netherlands Meteorological Institute (KNMI) (*van Meijgaard et al.*, 2008) are the RCMs selected to assess changes in precipitation and temperature over the IP along the 21st century. These RCMs were selected because they are regarded as the best-performing models at handling precipitation variability in other European regions, with RACMO2 performing best overall for the UK (*Simpson*, 2011, *van der Linden* and *Mitchell*, 2009; *Christensen et al.*, 2010; *Kjellström et al.*, 2010). We used the outputs from the RCMs driven by ERA-40 reanalysis for the period 1958–2002 to make comparisons with observed data and the same RCMs driven by associated global climate models (GCMs) for future projections covering the period 1951–2100. The ERA-40 reanalysis is produced by the European Centre for Medium-Range Weather Forecasting (ECMWF), and it is based on observed data such as conventional observations or satellite data among others. Temperature from the ERA-40 reanalysis is well simulated in the Northern Hemisphere when compared with mean observed sea-level pressure and geopotential 500hPa temperatures (*ECMWF*, 2004), and precipitation is well-handled in the Northern Hemisphere continents (*Bosilovich et al.*, 2008). In this study, KNMI-RACMO2 and DMI-HIRHAM5 are coupled with ECHAM5-r3 as a GCM, while HadRM3 is associated with HadCM3. The A1B climate change scenario was chosen to project the expected changes in precipitation and temperature over the IP as it represents a medium greenhouse gases forcing to the climate system according to IPCC AR-4 (*IPCC*, 2007).

The observed data has been extracted from the Monthly Iberian temperature and precipitation series (MITPS, *Fig. 1*). The MITPS dataset updates to 2010 the Spanish daily adjusted temperature/precipitation series (SDATS/SDAPS) and adds to its 22 stations two new data points to represent the western part of the IP (Portugal). The SDATS – and its MITPS update - was quality controlled (QC) following *Aguilar et al.*, (2002) and were homogenized by the Centre for Climate Change (C3) (*Brunet et al.*, 2006; *Brunet* et al., 2007) applying the standard normal homogeneity test (SNHT) (*Alexandersson* and *Moberg*, 1997). The two Portuguese series (Lisboa and Porto) have been subjected to quality control procedure of raw data and tested using homogenization procedure based on the standard normal homogeneity test, to detect and adjust most prominent inhomogeneities on a monthly scale.

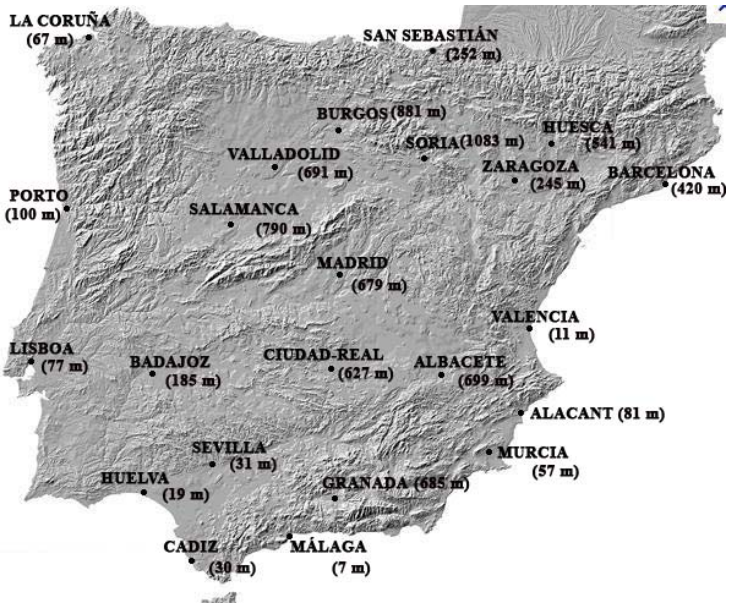

Fig. 1. MITPS station map: the closest city to each meteorological station is shown with the elevation (in brackets) of the last segment of record.

3. Methodology

The closest RCM grid box to each meteorological station has been selected to obtain the same geographical distribution of the Iberian simulated data according to observed data (MITPS) (*Fig. 1*). Monthly simulated precipitation and temperature data were obtained from DMI-HIRHAM5, HadRM3, and KNMI-RACMO2 model outputs driven by ERA-40 reanalysis and those driven by GCMs for each location. The RCMs outputs driven by ERA-40 reanalysis and by GCMs have been compared with the observed MITPS for the 1961–2010 period. All RCMs are more consistent when they are driven by ERA-40 reanalysis than by GCMs regarding precipitation and temperature simulation in the IP. Accumulated daily precipitation totals and mean temperature from observed and simulated data were totaled for Northern Hemisphere winter (DJF), spring (MAM), summer (JJA), and autumn (SON) seasons for the entire period. Based on the procedure applied by *Simpson* (2011), we computed the seasonal differences in precipitation totals, mean temperature, and the ratio between the standard deviations of simulated and observed data. Modeled and observed datasets have also been compared by computing the Pearson product-moment correlation coefficient and the root mean square error (RMSE). Finally, Kolmogorov-Smirnov test (K-S test) has been applied to evaluate the similarity between both statistical distributions.

Once the performance of the three RCMs is evaluated, simulations of seasonal precipitation and temperature from the RCMs driven by GCMs have been used to project the mean expected changes in precipitation and temperature over the IP for the periods 2011–2050 and 2051–2090 relative to 1961–2000 at seasonal time-scales under the A1B climate change scenario.

4. Results

4.1. Validation of the accuracy of precipitation simulations

The analysis of temperature and precipitation simulations showed quite different results, depending both on the model, the season of the year, and the different regions of the IP.

Precipitation simulations driven by ERA-40 tended to overestimate the observed data in central and north-western IP and also in the Ebro basin, especially in winter and spring (*Fig. 2*). Underestimated precipitation was found in the south, south-western IP and in the Mediterranean coast during all seasons, being more evident in summer and autumn. KNMI-RACMO2 showed the smallest deviations compared to observed data over the IP during all seasons except in summer, when it underestimated by between 20% and 40% of mean precipitation over most of the IP. HadRM3 produced overestimates of around 20–40% of mean precipitation in central, north-western area and in the Ebro basin, especially in spring and summer, and underestimated by 40% of mean precipitation in south-western areas and in the Mediterranean region for summer and autumn. DMI-HIRHAM5 showed large overestimates greater than 60% of mean precipitation in the Ebro basin and in the Sierra Nevada for winter and summer, respectively, and large underestimates towards 20–60% of mean precipitation for most of the IP, with higher anomalies located in the western and south-western area during all seasons.

Precipitation simulations from DMI-HIRHAM5 and KNMI-RACMO2 driven by ECHAM5-r3 and HadRM3 coupled with HadCM3 have also been compared with observed MITPS to check how the RCM simulations can be altered when they are driven by GCMs (*Fig. 3*). Large differences have been detected in mean seasonal precipitation from DMI-HIRHAM5 and KNMI-RACMO2 when they are driven by ERA-40 or by their associated GCMs (*Figs. 2* and *3*), but the simulations are closer in the case of HadRM3 in all seasons. All models have a tendency to overestimate mean precipitation in winter, spring, and autumn, while underestimates were found in summer. DMI-HIRHAM5 produced large overestimates greater than 80% of mean precipitation in central, north, and north-western IP for winter, spring, and autumn, while underestimates towards 20–40% of mean precipitation were focused in the south-western area and in the Mediterranean region for summer. HadRM3 and KNMI-RACMO2 overestimated by between 40–80% of mean precipitation in the Ebro basin and in the north-western IP mainly in winter and spring while underestimates around 40% of mean precipitation were primarily in the Mediterranean region for spring and summer. Note that large underestimates of greater than 60% of mean precipitation have been identified from KNMI-RACMO2 over most of the IP in summer.

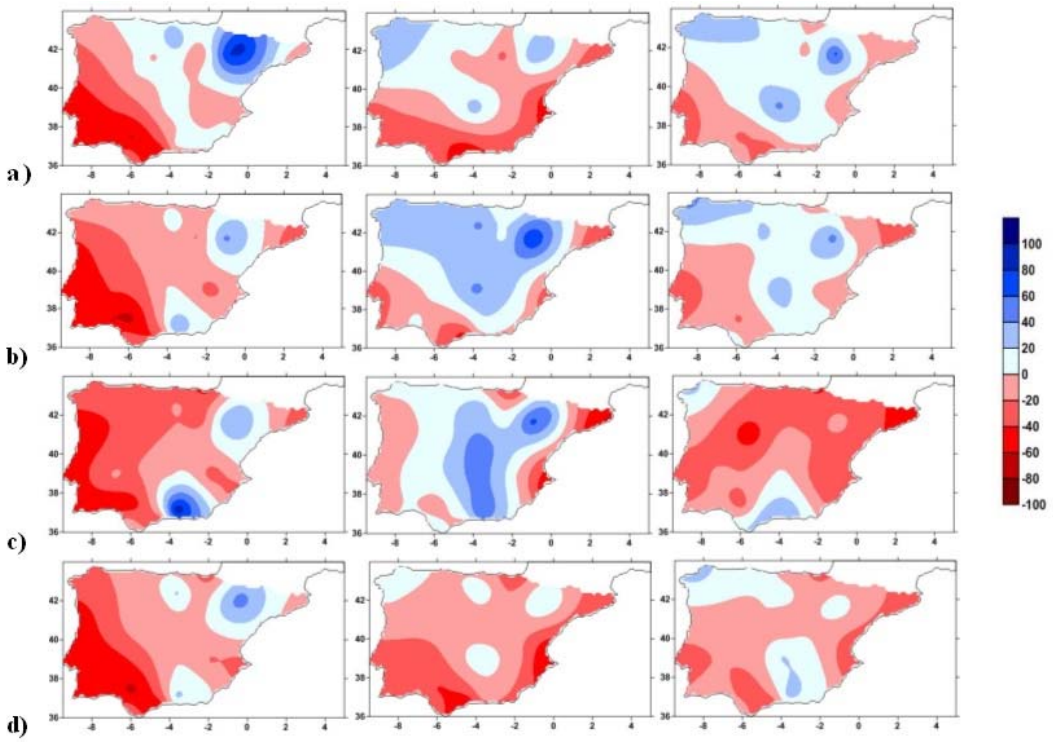

Fig. 2. Differences (in %) between simulated and observed mean seasonal precipitation totals (MITPS) in the IP for winter (DJF); **a)**, spring (MAM); **b)**, summer (JJA); **c)**, and autumn (SON); **d)** using the common period 1961–2000. The model outputs are derived from DMI-HIRHAM5 (left), HadRM3 (middle), and KNMI-RACMO2 (right), all driven by ERA-40 reanalysis.

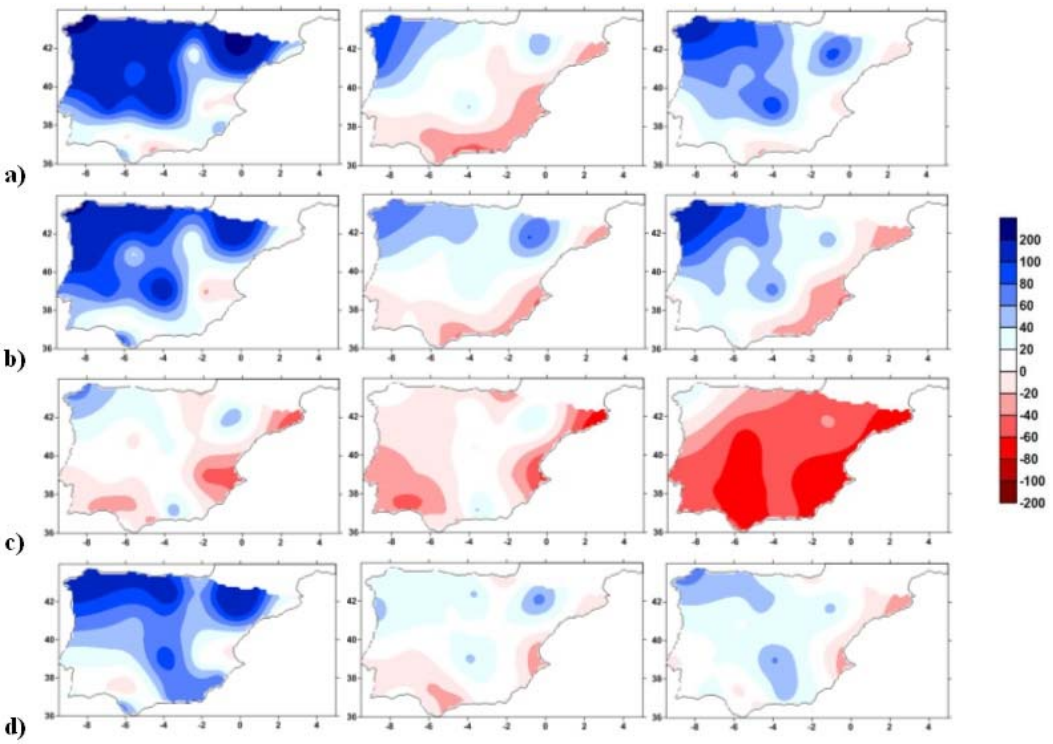

Fig. 3. Differences (in %) between simulated and observed precipitation seasonal totals (MITPS) in the IP for winter (DJF); **a)**, spring (MAM); **b)**, summer (JJA); **c)**, and autumn (SON); **d)** using the common period 1961–2000. The model outputs are derived from DMI-HIRHAM5 driven by ECHAM5-r3 (left), HadRM3 driven by HadCM3 (middle), and KNMI-RACMO2 driven by ECHAM5-r3 (right).

Simulated seasonal precipitation variability has been assessed from the ratio of standard deviations between mean simulated and observed precipitation from the three RCMs driven by ERA-40 reanalysis (*Fig. 4*). All RCMs exceeded 0.5 standard deviations for all seasons over most of the IP, while the ratio was greater than 1 standard deviation in some regions located in the north and central IP, especially for winter and spring. Otherwise, large differences in standard deviations could be appreciated from all RCMs driven by GCMs during all seasons (*Fig. 5*). All RCMs exceeded 1 standard deviation between mean simulated and observed precipitation over most of the IP, especially in spring and autumn.

The best correlations from the three RCMs driven by ERA-40 reanalysis between simulated and observed data were found in winter (*Fig. 6*), and the worst ones in summer with KNMI-RACMO2 the best-performing and DMI-HIRHAM5 second. The correlations were lower in the Mediterranean region than for the rest of the IP, especially in winter, summer, and autumn. Finally, the results from RMSE and K-S test (*Tables 1* and *2*) showed better fits between simulated and observed data using KNMI-RACMO2 during all seasons over most of the IP than DMI-HIRHAM5, which fitted better in the Mediterranean region.

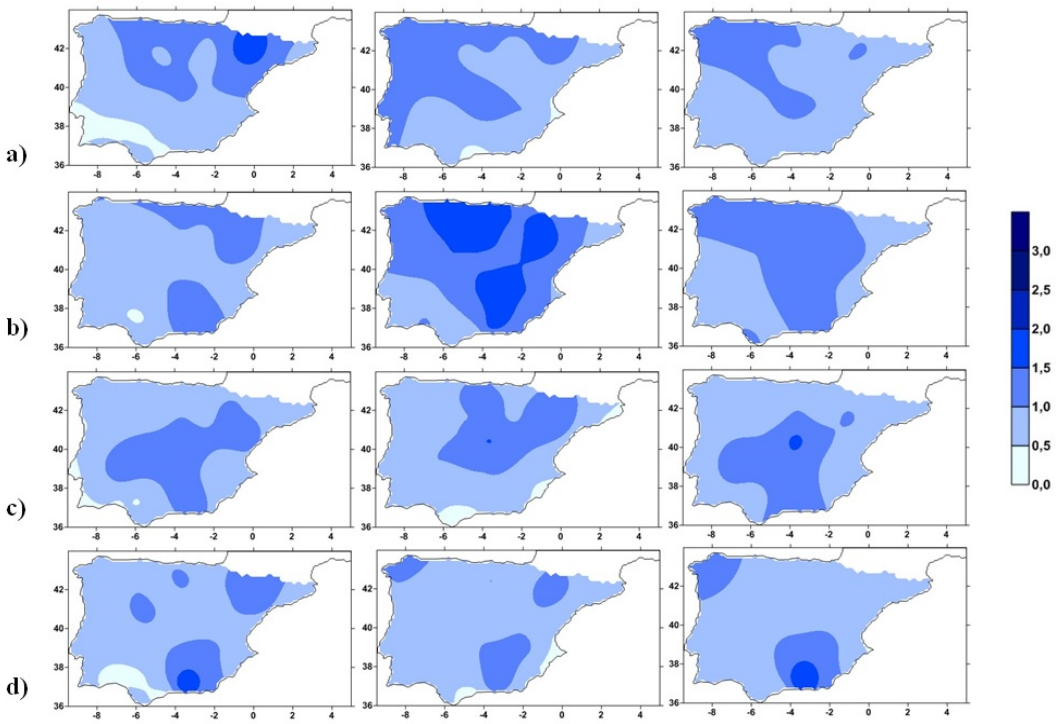

Fig. 4. Ratio of standard deviations between simulated and observed seasonal precipitation totals (MITPS) in the IP for winter (DJF); **a)**, spring (MAM); **b)**, summer (JJA); **c)**, and autumn (SON); **d)** using the common period 1961–2000. The model outputs are derived from DMI-HIRHAM5 (left), HadRM3 (middle), and KNMI-RACMO2 (right), all driven by ERA-40 reanalysis.

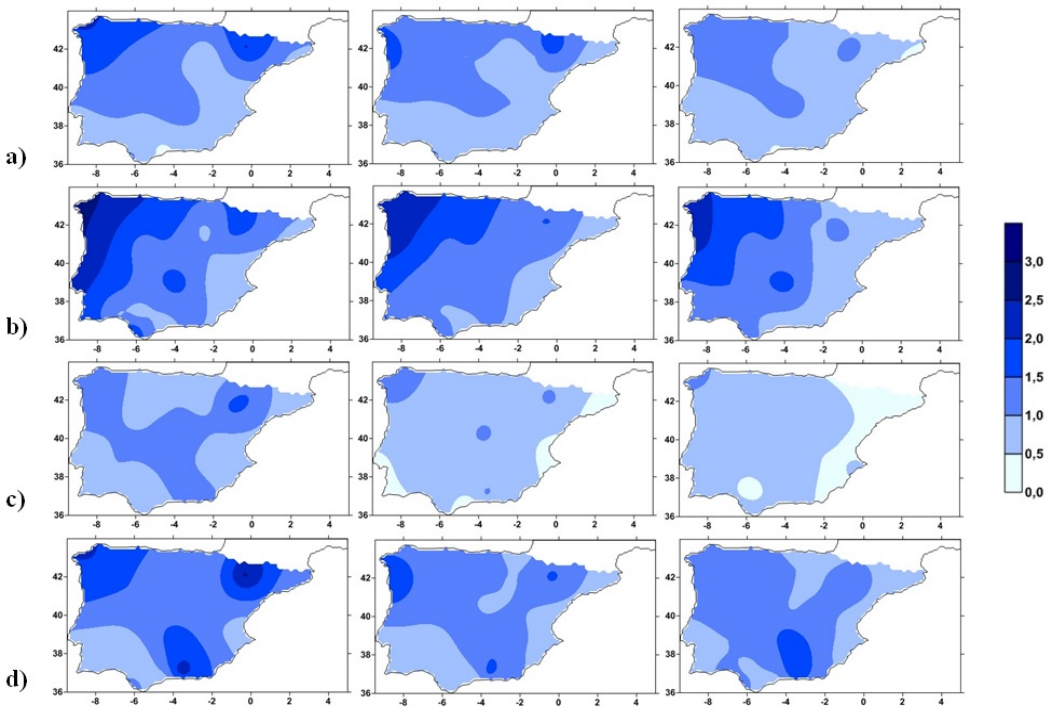

Fig. 5. Ratio of standard deviations between simulated and observed seasonal precipitation totals (MITPS) in the IP for winter (DJF); **a)**, spring (MAM); **b)**, summer (JJA); **c)**, and autumn (SON); **d)** using the common period 1961–2000. The model outputs are derived from DMI-HIRHAM5 driven by ECHAM5-r3 (left), HadRM3 driven by HadCM3 (middle), and KNMI-RACMO2 driven by ECHAM5-r3 (right).

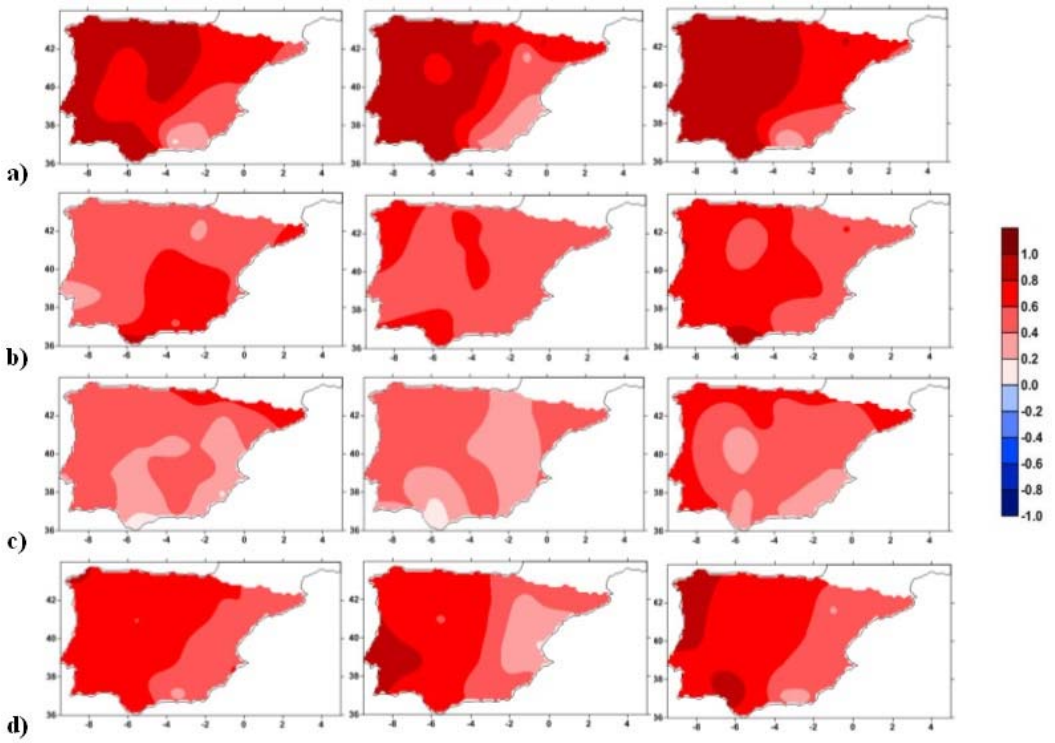

Fig. 6. Pearson Product-Moment Correlation coefficient between simulated and observed seasonal precipitation totals (MITPS) in the IP for winter (DJF); a), spring (MAM); b), summer (JJA); c), and autumn (SON); d) using the common period 1961–2000. The model outputs are derived from DMI-HIRHAM5 (left), HadRM3 (middle), and KNMI-RACMO2 (right), all driven by ERA-40 reanalysis. Correlations greater than 0.41 are statistically significant at the 99% level.

Table 1. Number of the best fitted RMSE values and K-S distances between simulated and observed precipitation and temperature for each season using the common period 1961–2000 for the 23 locations spread over the IP. The model outputs are derived from DMI-HIRHAM5, HadRM3, and KNMI-RACMO2, all driven by ERA-40 reanalysis. Values in bold refer to the maximum number of the best fitted values for each goodness of fit test and for the three RCMs assessed

		DMI-HIRHAM5		**HadRM3**		**KNMI-RACMO2**	
	Seasons	**Nº RMSE**	**Nº K-S distances**	**Nº RMSE**	**Nº K-S distances**	**Nº RMSE**	**Nº K-S distances**
Precipitation	Winter (DJF)	4	**10**	3	3	**16**	**10**
	Spring (MAM)	10	7	0	6	**13**	**10**
	Summer (JJA)	4	5	6	7	**13**	**11**
	Autumn (SON)	5	5	3	4	**15**	**14**
Temperature	Winter (DJF)	**14**	**14**	3	3	6	6
	Spring (MAM)	**15**	**14**	4	6	4	3
	Summer (JJA)	4	4	6	5	**13**	**14**
	Autumn (SON)	**11**	8	7	**11**	5	4

Table 2. Averaged RMSE values and averaged K-S distances between simulated and observed precipitation and temperature over the whole IP for each season using the common period 1961–2000. The model outputs are derived from DMI-HIRHAM5, HadRM3, and KNMI-RACMO2, all driven by ERA-40 reanalysis. Values in bold refer to the best fitted values for each goodness of fit test and for the three RCMs assessed

		DMI-HIRHAM5		**HadRM3**		**KNMI-RACMO2**	
	Seasons	**RMSE**	**K-S distances**	**RMSE**	**K-S distances**	**RMSE**	**K-S distances**
Precipitation	Winter (DJF)	92.69	0.29	81.45	0.28	**67.25**	**0.23**
	Spring (MAM)	69.33	0.35	77.63	0.32	**59.19**	**0.26**
	Summer (JJA)	46.02	0.35	48.91	0.33	**43.83**	**0.31**
	Autumn (SON)	97.19	0.33	90.85	0.31	**78.40**	**0.25**
Temperature	Winter (DJF)	**1.37**	**0.50**	1.65	0.58	1.76	0.58
	Spring (MAM)	**1.05**	**0.40**	1.27	0.46	1.52	0.57
	Summer (JJA)	1.65	0.59	1.88	0.59	**1.34**	**0.49**
	Autumn (SON)	**1.13**	0.43	1.25	**0.42**	1.57	0.61

From the results obtained above, KNMI-RACMO2 is the most suitable RCM for simulating precipitation in the IP when driven by ERA-40 data and by GCMs, although large uncertainties in mean precipitation should be appreciated for summer. All RCMs, including KNMI-RACMO2, are still affected by uncertainties in mean precipitation that have to be taken into account for future projections especially when the RCMs are driven by GCMs.

4.2. Validation of the accuracy of temperature simulations

The outputs from the RCMs driven by ERA-40 reanalysis and driven by GCMs for temperature were also compared with observed MITPS for each location applying the methodology described earlier for the common period 1961–2000 at seasonal time-scale.

Simulations of the RCMs driven by ERA-40 showed a bias in mean seasonal temperature relative to observed MITPS towards overestimates in north-eastern IP for winter and autumn and central IP, especially in summer (*Fig. 7*). Additionally, underestimates were detected in the north and north-western IP, especially in winter, spring, and autumn and in the south-eastern IP in summer. DMI-HIRHAM5 showed the smallest anomalies of 1 ºC of mean simulated temperature in most of the IP during all seasons with HadRM3 the second best. DMI-HIRHAM5 overestimated between 2–3 ºC of mean temperature mainly in north-eastern IP for winter and autumn and greater than 3 ºC in central IP for summer. Underestimates of between 2–3 ºC of mean temperature were focused in the north and north-western area in winter, spring, and autumn, while in the south-eastern IP, similar underestimates were found for summer. HadRM3 produced overestimates of between 3–4 ºC of mean temperature in the central and in north-eastern corner of the IP (around 2 ºC) in winter and summer, respectively, while underestimates of between 1–3 ºC were identified in the central, north, and north-western areas during winter, spring, and autumn. KNMI-RACMO2 showed overestimates of around 2 ºC for mean temperature in the central IP only for summer, but underestimates were detected in the most of the IP, but were more prominent (between 3–4 ºC) in the north-western area in winter, spring, and autumn.

Additionally, temperature simulations from the RCMs coupled with associated GCMs were compared with observed MITPS in order to see whether RCM simulations are affected when they are driven by GCMs (*Fig. 8*). Some differences have been detected in mean seasonal temperature from DMI-HIRHAM5 and HadRM3 when they are driven by ERA-40 or by their associated GCMs (*Figs. 7* and *8*), but the simulations fitted better in the case of KNMI-RACMO2 driven by the associated GCM than those driven by ERA-40 in all seasons. All models have a tendency to overestimate by between 1–2 ºC of mean temperature in the Mediterranean region in winter, while underestimates of between 1–2 ºC for mean temperature were found in most of the IP, but were

more prominent in the north-western area during winter, spring, and autumn. DMI-HIRHAM5 showed overestimates of around 2–3 ºC in the Mediterranean region for winter and autumn, while the underestimates of 2–3 ºC were located in the central, north, and north-western parts of the IP in spring and summer. HadRM3 and KNMI-RACMO2 produced similar underestimates of 2–3 ºC over most of the IP, mainly located in the north-western corner during winter, spring, and autumn.

Seasonal temperature variability has been figured out from the ratio of standard deviations between simulated and observed average temperatures from the three RCMs driven by ERA-40 reanalysis (*Fig. 9*). All RCMs exceeded 0.5 standard deviations over the IP for all seasons being greater than 1 standard deviation over most of the IP according to HadRM3. The seasonal temperature variability between simulated and observed data from the RCMs driven by GCMs produced similar differences than the simulations driven by ERA-40 (*Fig. 10*). All RCMs exceeded 0.5 standard deviations over the whole IP during all seasons with a ratio greater than 1 standard deviation for spring, summer, and autumn according to HadRM3.

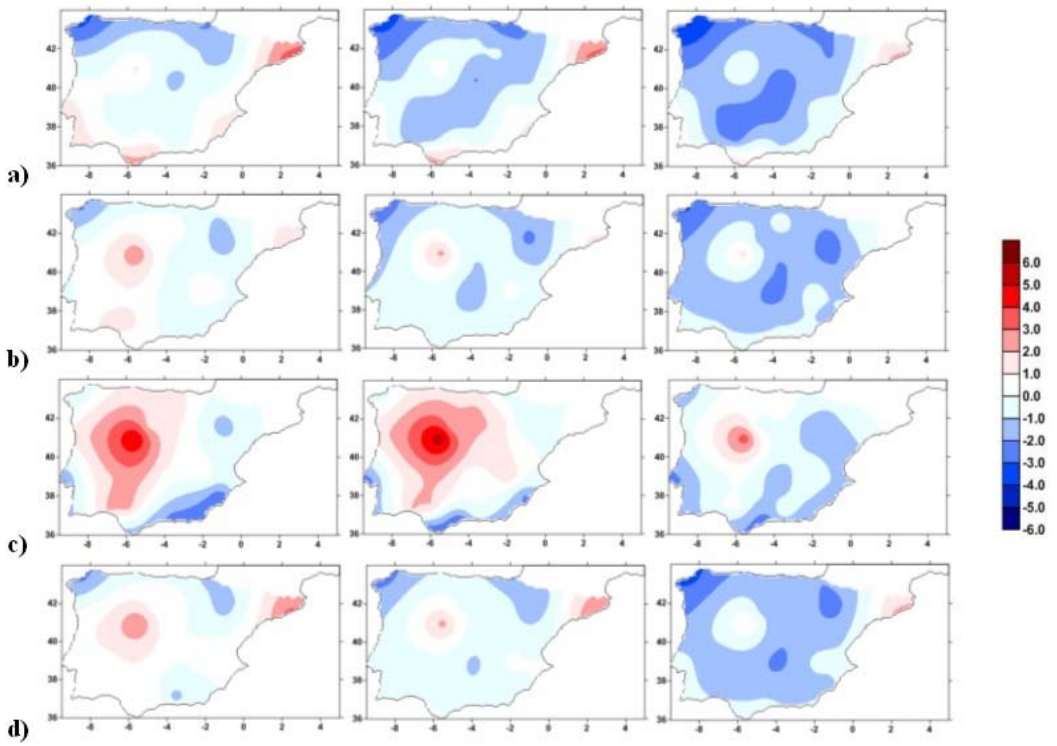

Fig. 7. Differences (in ºC) between simulated and observed seasonal average temperatures (MITPS) in the IP for winter (DJF); **a)**, spring (MAM); **b)**, summer (JJA); **c)**, and autumn (SON); **d)** using the common period 1961–2000. The model outputs are derived from DMI-HIRHAM5 (left), HadRM3 (middle), and KNMI-RACMO2 (right), all driven by ERA-40 reanalysis.

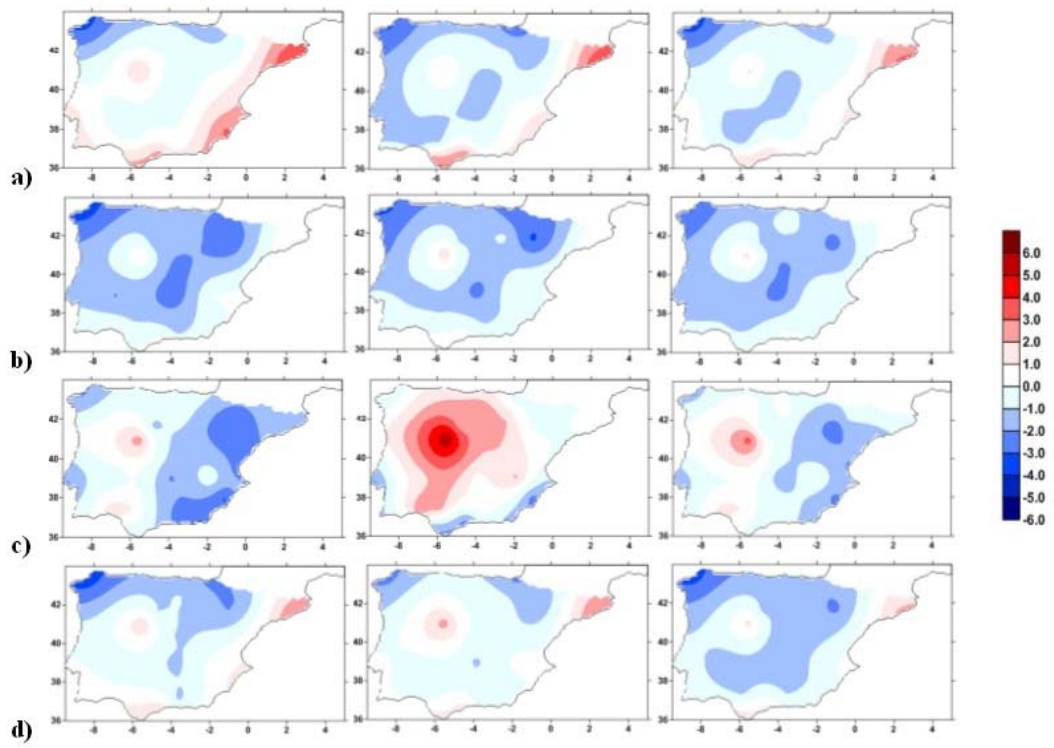

Fig. 8. Differences (in ºC) between simulated and observed seasonal average temperatures (MITPS) in the IP for winter (DJF); **a)**, spring (MAM); **b)**, summer (JJA); **c)**, and autumn (SON); **d)** using the common period 1961–2000. The model outputs are derived from DMI-HIRHAM5 driven by ECHAM5-r3 (left), HadRM3 driven by HadCM3 (middle), and KNMI-RACMO2 driven by ECHAM5-r3 (right).

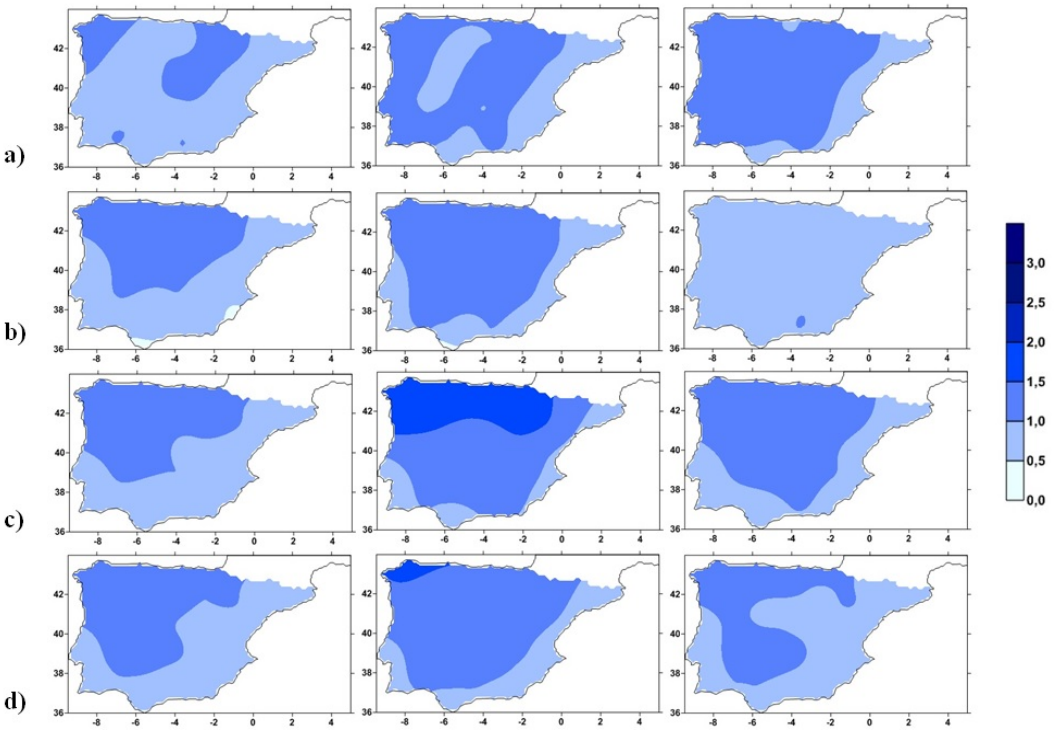

Fig. 9. Ratio of standard deviations between simulated and observed seasonal average temperatures (MITPS) in the IP for winter (DJF); **a)**, spring (MAM); **b)**, summer (JJA); **c)**, and autumn (SON); **d)** using the common period 1961–2000. The model outputs are derived from DMI-HIRHAM5 (left), HadRM3 (middle), and KNMI-RACMO2 (right), all driven by ERA-40 reanalysis.

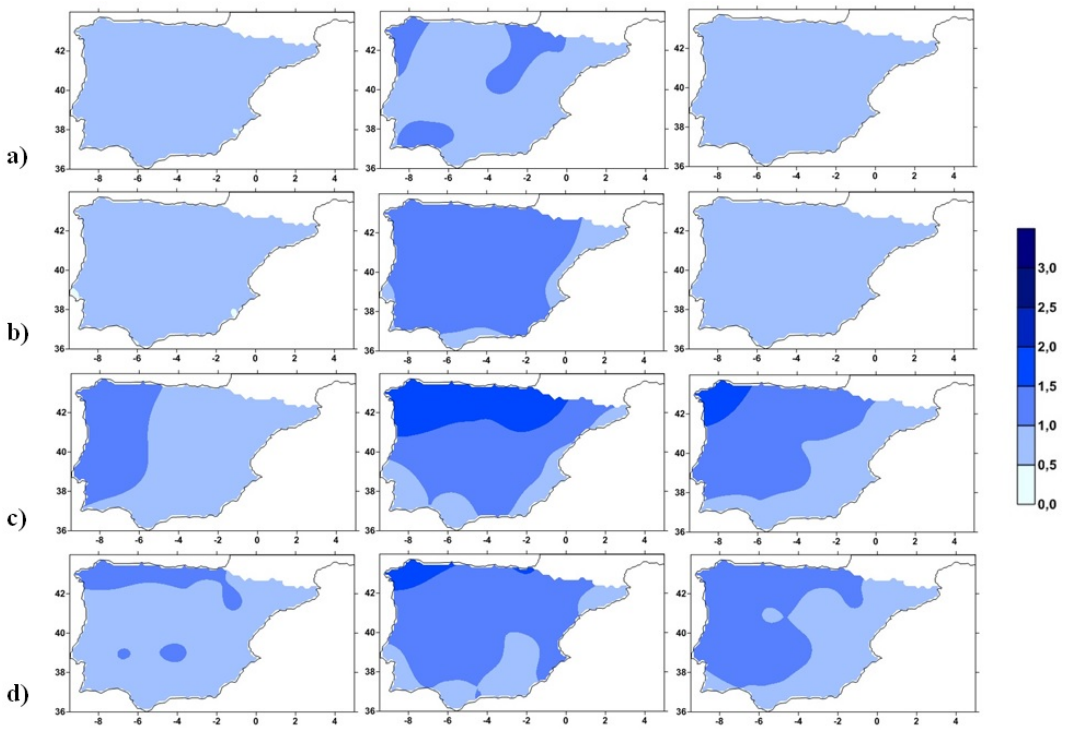

Fig. 10. Ratio of standard deviations between simulated and observed seasonal average temperatures (MITPS) in the IP for winter (DJF); **a)**, spring (MAM); **b)**, summer (JJA); **c)**, and autumn (SON); **d)** using the common period 1961–2000. The model outputs are derived from DMI-HIRHAM5 driven by ECHAM5-r3 (left), HadRM3 driven by HadCM3 (middle), and KNMI-RACMO2 driven by ECHAM5-r3 (right).

The three RCMs driven by ERA-40 reanalysis showed very high correlations between simulated and observed data during all seasons with DMI-HIRHAM5 the best-performing overall, although the correlations are lower in the Mediterranean region than in the rest of the IP, especially in summer and autumn (*Fig. 11*). Finally, the results from RMSE and K-S test showed a better fit between simulated and observed data using DMI-HIRHAM5 during winter and spring over most IP, while KNMI-RACMO2 fitted better in summer (see *Tables 1* and *2*).

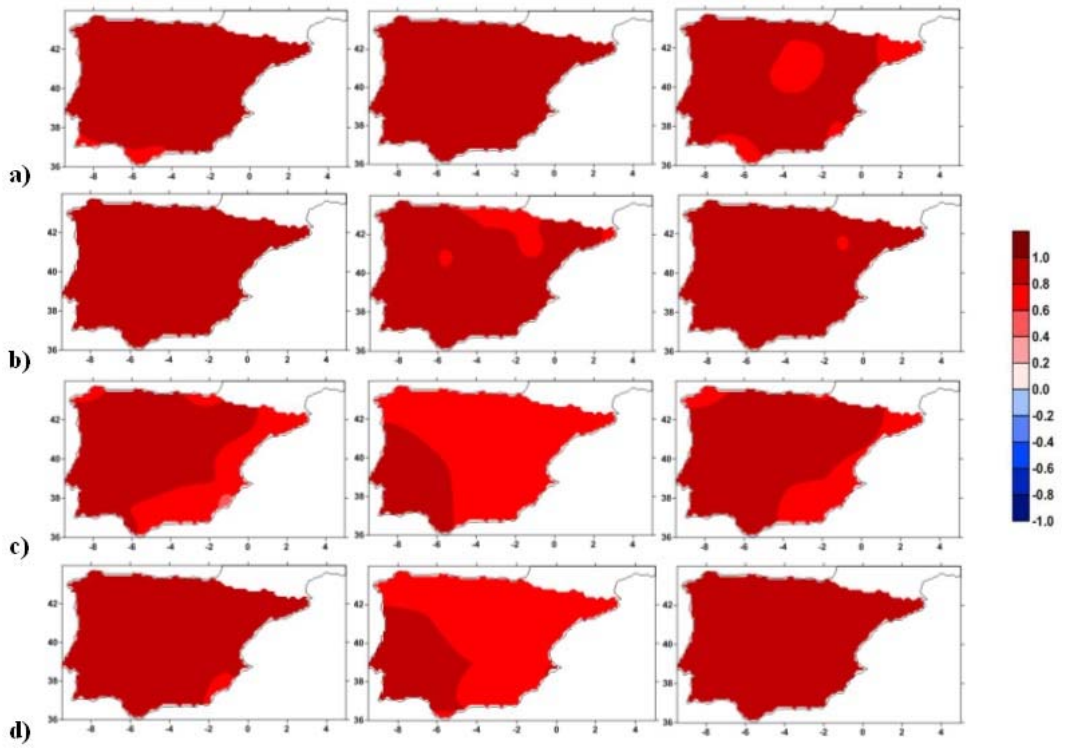

Fig. 11. Pearson product-moment correlation coefficient between simulated and observed seasonal average temperatures (MITPS) in the IP for winter (DJF); **a)**, spring (MAM); **b)**, summer (JJA); **c)**, and autumn (SON); **d)** using the common period 1961–2000. The model outputs are derived from DMI-HIRHAM5 (left), HadRM3 (middle), and KNMI-RACMO2 (right), all driven by ERA-40 reanalysis. Correlations greater than 0.34 are statistically significant at the 99% level.

From the measures considered above, DMI-HIRHAM5 is the best RCM of the three tested for the IP for simulating temperature, although large uncertainties are affecting RCMs, especially when they are driven by GCMs. These uncertainties should be considered when projecting temperature over the IP along the 21st century.

4.3. Projected changes in mean seasonal precipitation

The outputs from DMI-HIRHAM5 and KNMI-RACMO2 driven by ECHAM5-r3 and HadRM3 driven by HadCM3 were used to assess the projected changes in mean seasonal precipitation in the IP for the periods 2011–2050 (*Fig. 12*) and 2051–2090 (*Fig. 13*) relative to 1961–2000 under the A1B climate change scenario.

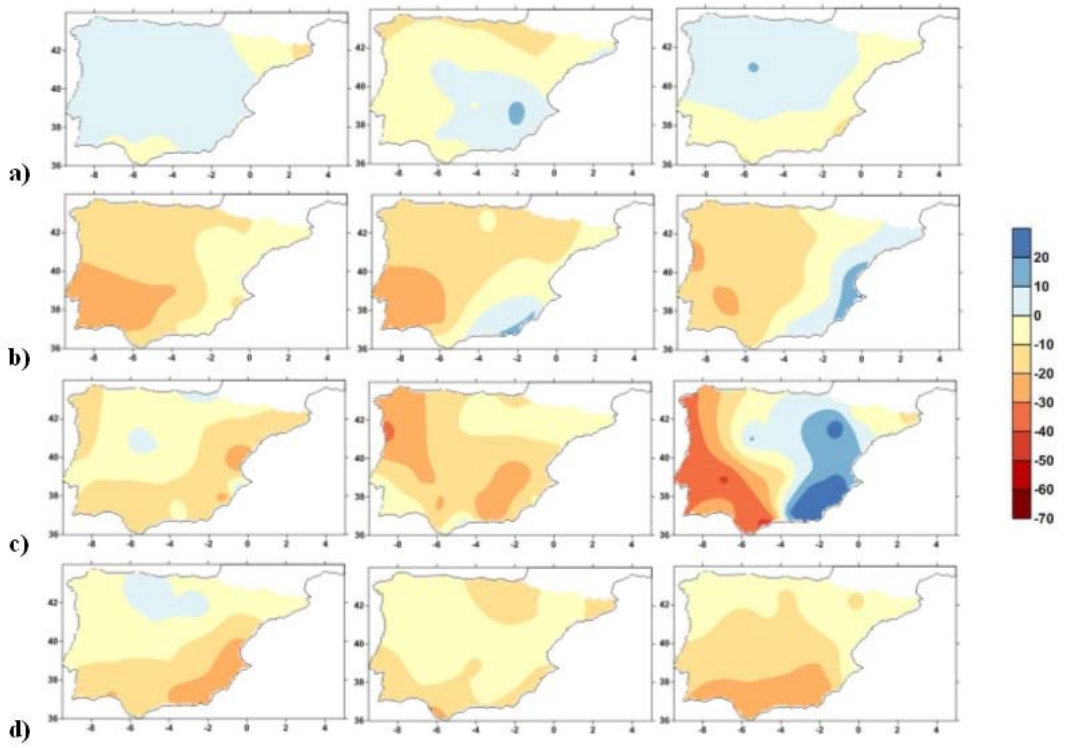

Fig. 12. Seasonal precipitation change (in %) projected for the period 2011–2050 relative to 1961–2000 in the IP for winter (DJF); **a)**, spring (MAM); **b)**, summer (JJA); **c),** and autumn (SON); **d)** using the model outputs derived from DMI-HIRHAM5 driven by ECHAM5-r3 (left), HadRM3 driven by HadCM3 (middle), and KNMI-RACMO2 driven by ECHAM5-r3 (right).

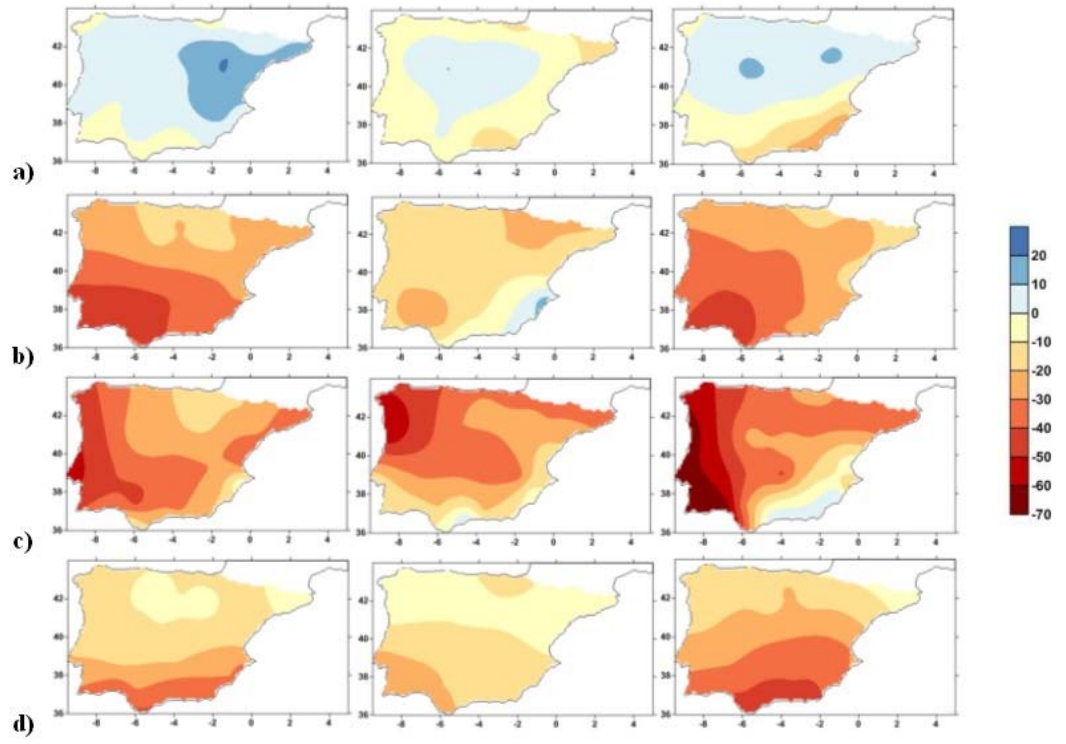

Fig. 13. Seasonal precipitation change (in %) projected for the period 2051–2090 relative to 1961–2000 in the IP for winter (DJF); **a)**, spring (MAM); **b)**, summer (JJA); **c),** and autumn (SON); **d)** using the model outputs derived from DMI-HIRHAM5 driven by ECHAM5-r3 (left), HadRM3 driven by HadCM3 (middle), and KNMI-RACMO2 driven by ECHAM5-r3 (right).

Model outputs agree on a future decrease in precipitation over most of the IP during the 21st century for spring, summer, and autumn, although no clear signal was found for winter. All RCM simulations projected a clear decrease of 10–20% in mean precipitation for spring, summer, and autumn across most of the IP for the period 2011–2050 relative to 1961–2000 (*Fig. 12*). DMI-HIRHAM5 and KNMI-RACMO2 outputs projected similar decrease in mean precipitation of 30–50% for spring and summer over most of the IP by the 2051–2090 period, while a decline of 20–30% was detected in autumn (*Fig. 13*). HadRM3 simulations showed smaller decreases in mean precipitation of 10–20% in spring and autumn, and around 20–30% increases in summer for the mid-late century. No clear signal was found in mean winter precipitation from all the RCM outputs for both time-periods (*Figs. 12* and *13*).

In particular, DMI-HIRHAM5 and KNMI-RACMO2 outputs agree on an increase in mean winter precipitation of 5–10% in central, north, and north-western IP, and a decrease of 10% in the south, south-eastern, and in the Mediterranean region for the period 2011–2050 declining by between 10–20% by the 2051–2090 period (*Figs. 12* and *13*, respectively). All RCM outputs showed a decrease in mean spring precipitation of 10–20% for most of the IP for the period 2011–2050, although HadRM3 and KNMI-RACMO2 produced precipitation increases of 10% in some areas of the Mediterranean and south-eastern coasts of the IP. An evident spring precipitation decrease of 20–40% has been projected from all RCMs for the whole IP by the 2051–2090 period being more extreme in the south and south-western areas than in the central and in the north. DMI-HIRHAM5 produced a clear decrease of 10–20% of mean summer precipitation over most of the IP for the period 2011–2050, but declining to 20–50% by the 2051–2090 period, especially in the west and south-western area. HadRM3 showed a decline of 10–30% (2011–2050) and of 20–60% in mean summer precipitation more evident in the north and north-western IP than in the south-eastern and south-western areas. KNMI-RACMO2 projected a decrease of 10–40% in summer precipitation (2011–2050) in the west and south-western area becoming 20–70% over most IP by the 2051–2090 period. Despite this, precipitation increases were found from KNMI-RACMO2 outputs in the south-eastern area of 10–60% (2011–2050) and of 5% (2051–2090). Finally, all RCM simulations showed a clear decline in mean autumn precipitation of 10–20% (2011–2050) and of 10–40% (2051–2090) for the whole IP being more extreme in the southern than in the northern area.

4.4. Projected changes in mean seasonal temperature

The model outputs associated with their GCMs were also used to assess the projected changes in mean seasonal temperature for the IP using the periods 2011–2050 (*Fig. 14*) and 2051–2090 (*Fig. 15*) relative to 1961–2000 under the A1B climate change scenario.

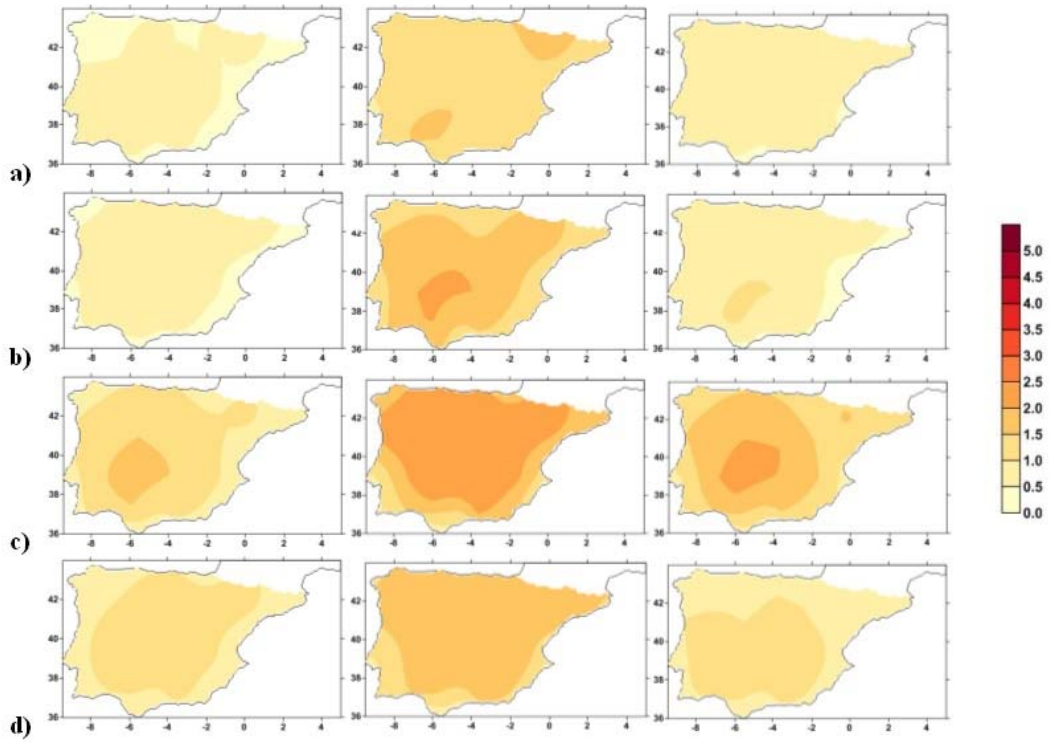

Fig. 14. Seasonal temperature change (in ºC) projected for the period 2011–2050 relative to 1961-2000 in the IP for winter (DJF); **a)**, spring (MAM); **b)**, summer (JJA); **c),** and autumn (SON); **d)** using the model outputs derived from DMI-HIRHAM5 driven by ECHAM5-r3 (left), HadRM3 driven by HadCM3 (middle), and KNMI-RACMO2 driven by ECHAM5-r3 (right).

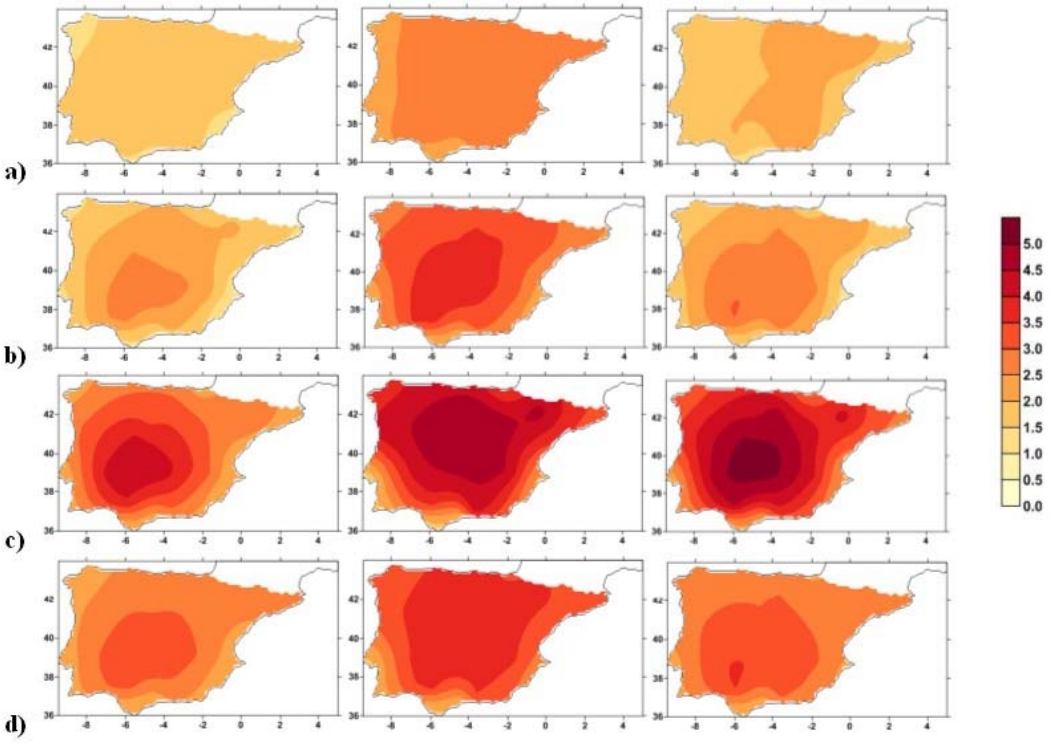

Fig. 15. Seasonal temperature change (in ºC) projected for the period 2051–2090 relative to 1961-2000 in the IP for winter (DJF); **a)**, spring (MAM); **b)**, summer (JJA); **c),** and autumn (SON); **d)** using the model outputs derived from DMI-HIRHAM5 driven by ECHAM5-r3 (left), HadRM3 driven by HadCM3 (middle), and KNMI-RACMO2 driven by ECHAM5-r3 (right).

A clear increase in mean seasonal temperature has been projected from all RCM simulations over the whole IP along the year for the periods 2011–2050 and 2051–2090 relative to 1961–2000 (*Figs 14* and *15*). The highest rates were focused in summer and autumn in both time-periods, and the lowest rates were found in winter and spring. DMI-HIRHAM5 and KNMI-RACMO2 outputs showed a 0.5 ºC increase in mean temperatures for winter and spring using the period 2011–2050 with higher rates of 1.5–2 ºC by the 2051–2090 period for the whole IP. Both RCMs produced an increase of 1–1.5 ºC in summer and of 1 ºC in autumn for the period 2011–2050, while they projected an increase of 3–5 ºC in summer and of 2.5–3.5 ºC in autumn by the 2051–2090 period. HadRM3 simulations showed increases of 1.5 ºC for winter, of 1.5–2 ºC for spring and autumn, and of 2–2.5 ºC in summer for the period 2011–2050, while by the 2051–2090 period the increases reached 3 ºC in winter, 3–4 ºC in spring and autumn, and 3.5–4.5 ºC in summer.

All RCM simulations concurred in producing higher rates of change in mean temperatures over the continental IP including the Ebro basin, the Central System, the North and South Plateaus, and the south-western area for all seasons, but especially in summer and autumn. Otherwise, the smallest anomalies were found along the coastline, but especially in the north and north-western coast. In this way, RCM simulations suggested that the continental effect in temperatures will play a major role over the IP along the 21st century reaching extreme temperature increases in the interior area, especially in summer.

5. Discussion and conclusions

In this study, three regional climate models obtained from the EU-Ensembles project have been used to assess projected changes in mean seasonal precipitation and temperature over the whole IP under the A1B climate change scenario for the 21st century. These RCMs were the best-performing models for simulating precipitation and temperature for Europe according to *van der Linden* and *Mitchell* (2009), *Christensen et al.*, (2010), and *Kjellström et al.*, (2010).

The RCM outputs driven by ERA-40 reanalysis have been compared directly with observed MITPS to test the reliability of the simulations. According to the measures tested in this study, KNMI-RACMO2 is the best RCM for simulating precipitation in the IP being consistent with the results obtained by *Simpson* (2011) for UK precipitation, although some problems in summer precipitation should be appreciated. DMI-HIRHAM5 is the best regional climate model for simulation of temperature in the IP. The RCM comparisons with observed data are a necessary, but not sufficient condition to test the accuracy of the models, because current climate change can modify the original basis for a reliable simulation of past climate conditions.

Simulations of seasonal precipitation and temperature from the RCMs driven by GCMs have been used to project the mean expected changes for the periods 2011–2050 and 2051–2090 relative to 1961–2000. Large differences have been detected between RCM outputs coupled with associated GCMs and the observed MITPS. This produces large uncertainties in the results, and these have to be taken into account when assessing model outputs (*Blenkinsop et al.*, 2007; *Sheffield* and *Wood*, 2008; *Rammukainen*, 2010; *Mishra*, 2011; *IPCC*, 2012). Despite, all RCM simulations are projecting a clear decrease of 10% in mean precipitation for spring, summer, and autumn in most IP for the period 2011–2050, it is more evident in the southern than in the northern area. A significant decrease of 20–40% in mean precipitation is expected by the 2051–2090 period for the same seasons, while no clear signal was found in mean winter precipitation from all the RCM outputs and for both time-periods. Model outputs have also shown an increase in mean temperatures between 0.5–1.5 ºC for winter and spring for the period 2011–2050 with higher rates of 1.5–2.5 ºC and 1.5–3 ºC, respectively, by the 2051–2090 period. An increase of between 1–2 ºC was found in summer and 1–1.5 ºC in autumn for the period 2011–2050 being higher by the 2051–2090 period (3–4 ºC in summer and 2.5–3.5 ºC in autumn). Moreover, all RCM simulations concurred by finding higher rates of change in mean temperatures over the continental IP, and the smallest anomalies were found along the coastline, but especially in the north and north-western coasts. In this way, RCM simulations suggested that the continental effect in temperatures will be enhanced and will play a major role in producing extreme temperature increases in the interior area, especially in summer. These findings are consistent with the results obtained by *Gómez-Navarro et al.*, (2010), *Rodríguez-Puebla* and *Nieto*, (2010), and *Jerez et al.*, (2012), and *Jerez* and *Montavez* (2012) for the IP along the 21st century.

The decrease in mean precipitation and the increase in mean temperature projected from the model outputs in the IP could worse current drought conditions for the second half of the 21st century, especially in summer.

Acknowledgements: The authors acknowledge the contribution of *Mª Antonia Valente* and *Ricardo Trigo* from the Climatology and Climate Change Research Group of the Instituto *Dom Luiz*, Lisbon University, to provide us climatic data of Portugal (Porto and Lisboa time series). Original and updated Spanish daily data not included in SDATS and SDAPS were obtained from AEMET servers. Monthly simulated temperature and precipitation data from the three regional climate models driven by ERA-40 reanalysis and driven by GCMs were obtained from the EU-Ensembles project.

References

Aguilar, E., Brunet, M., Saladié, O., Sigró, J., and *López, D.,* 2002: Hacia una aplicación optima del standard normal homogeneity test para la homogeneización de series de temperatura. In (Eds.:*Cuadrat JM, Vicente SM, SAZ MA)* La Información Climática Como Herramienta de Gestión Ambiental. VII Reunión Nacional de Climatología, Grupo de Climatología de la AGE, Universidad de Zaragoza: Zaragoza, 17–33. (In Spain)

Alexandersson, H. and *Moberg, A.*,1997: Homogenisation of Swedish temperature data, Part I: Homogeneity test for linear trends, *Int. J. Climatol. 17*, 25–34.

Barrera-Escoda, A., 2008. Evolución de los extremos hídricos en Catalunya en los últimos 500 años y su modelización regional (Evolution of hydric extremes in Catalonia during the last 500 years and its regional modelling), Ph.D. Thesis, Internal Publication, University of Barcelona, Barcelona, Spain. (In Spain)

Beniston, M., Stephenson, D.B., Christensen, O.B., Ferro, C.A.T., Frei, C., Goyette, S.,Halsnaes, K., Holt, T., Jylha, K., Koffi, B., Palutikof, J., Scholl, R., Semmler, T., and *Woth, K., 2007:* Future extreme events in Eurpoean climate: an exploration of regional climate model projections. *Climatic Change 81*, 71–95.

Bosilovich, M.G., Chen, J., Robertson, F.R., Adler, R.F., 2008: Evaluation of Global Precipitation in Reanalysis. *J. Appl. Meteorol. Climatol. 47*, 2279–2299.

Blenkinsop, S. and Fowler, H.J., 2007: Changes in European drought characteristics projected by the PRUDENCE regional climate models. *Int. J. Climatol. 27*, 1595–1610.

Brunet, M., Jones, P.D., Sigró, J., Saladié, O., Aguilar, E., Moberg, A., Della-Marta, P.M., Lister D., Walther, A., and *López, D.*, 2007: Temporal and spatial temperature variability and change over Spain during 1850-2005. *J. Geophys. Res.-Atmos. 112*:D12117.

Brunet, M., Saladié, O., Jones, P.D., Sigró, J., Aguilar, E., Moberg, A., Walther, A., Lister, D., López, D., and *Almarza, C.*, 2006: The development of a new daily adjusted temperature dataset for Spain (1850–2003). . *Int. J. Climatol. 26*,1777–1802.

Christensen, J.H., Kjellström, E., Giorgi, F., Lenderink, G., and *Rammukainen, M.*, 2010: Weight assignment in regional climate models. *Climate Res. 44*, 179–194.

Christensen, J.H. and *Christensen, O.B.*, 2007: A summary of the PRUDENCE model projections of changes in European climate during this century. *Climatic Change 81*(S1), 7–30.

CLIVAR Assessment, 2010: Clima en España: Pasado presente y futuro. In (Eds. *Pérez F, Boscolo R,*) www.clivar.es (Last visit: 23-02-2013).

Collins, W.J., Bellouin, N., Doutriaux-Boucher, M., Gedney, N., Hinton, T., Jones, C.D., Liddicont, S., Martin, G., O'Connor, F., Rae, J., Senior, C., Totterdell, I., Woodward, S., Reichler, T., Kin, J., 2010: Evaluation of the HadGEM2 model. *Met Office Hadley Centre. Technical Note no. HCTN 74*, available from Met Office, FitzRoy Road, Exeter, UK. EX1 3PB.

Dai, A., 2011. Drought under global warming: A review. *Wiley Interdisciplinary Reviews:Climate Change 2*, 45–65.

Dai, A., 2012. Increasing drought under global warming in observations and models. *Nature Climate Change 3, 53–58.*

ECMWF 2004. ERA-40: ECMWF 45-year reanalysis o the global atmosphere and surface conditions 1957–2002. *ECMWF Newsletter Nº. 101*. Retrieved 5th November, 2010; http://www.mad.zmaw.de/uploads/media/e40Overwiew.pdf.

Gomez-Navarro, J.J., Montavez, J.P., Jimenez-Guerrero, P., Jerez, S., Garcia-Valero, J.A., Gonzalez-Rouco, J.F., 2010: Warming patterns in regional climate change projections over the Iberian Peninsula. *Meteorol. Z. 19*, 275–285.

IPCC climate change 2012: Managing the Risks of Extreme Events and Disasters to Advance Climate Change Adaptation. A Special Report of Working Groups I and II of the Intergovernmental Panel on Climate Change. *(Eds. Field, C.B., V. Barros, T.F. Stocker, D. Qin, D.J. Dokken, K.L. Ebi, M.D. Mastrandrea, K.J. Mach, G.-K. Plattner, S.K. Allen, M. Tignor, and P.M. Midgley)*, Cambridge University Press, Cambridge, UK, and New York, NY, USA, 582.

IPCC climate change 2007: the physical science basis. In: (E*ds .Salomon S, Qin D, Manning M, Chen Z, Marquis M, Averyt KB, Tignor M, Miler HL,)* Contribution of Working Group I to the Fourth Assessment Report of the International Panel on Climate Change Program. Cambridge, UK/New York, USA: Cambridge University Press; 2007, 996.

Jerez, S., Montavez, J.P., Gomez-Navarro, J.J., Jimenez, P.A., Jimenez-Guerrero, P., Lorente-Plazas, R., Gonzalez-Rouco, J.F., 2012: The role of the land-surface model for climate change projections over the Iberian Peninsula. *J. Geophys. Res. 117*, D01,109.

Jerez, S. and *Montavez, J.P.*, 2012: A multi-physics ensemble of regional climate change projections over the Iberian Peninsula. *Clim. Dynam.* DOI: 10.1007/s00382-012-1551-5.

Kjellström, E., Boberg, F., Castro, M., Christensen, JH., Nikulin, G., and *Sanchez, E.,* 2010. Daily and monthly temperature and precipitation statistics as performance indicators for regional climate models. *Climate Res. 44*, 121–134.

van der Linden and *Mitchell, J.F.B.,* 2009: ENSEMBLES: Climate Change and its Impacts: Summary of research and results from the ENSEMBLES project. Met Office Hadley Centre, FitzRoy Road, Exeter EX1 3PB, UK.

Mariotti, A., Zeng, N., Yoon, J.H., Artale, V., Navarra, A., Alpert, P., and Li, L.Z.X., 2008: Mediterranean water cycle changes: transition to drier 21st century conditions in observations and CMIP3 simulations. *Environ. Res. Letters, 3*, 044001.

Mishra, A.K. and *Singh, V.P.,* 2011: Drought modeling-A review. *J. Hydrol. 403*, 157–175.

Rammukainen, M., 2010: State-of-the-art with regional climate models. *Wiley Interdisciplinary Reviews: Climate Change 1*, 82–96.

Rodríguez-Puebla, C. and *Nieto, S.,* 2010. Trends of precipitation over Iberian Peninsula and the North Atlantic Oscillation under climate change conditions. *Int. J. Climatol. 30*, 1807–1815.

Sánchez, E., Gaertner, M.A., Gallardo, C., 2009: Regionalización diaria de la precipitación diaria sobre la Península Ibérica: análisis de la resolución espacial en la descripción del clima actual y clima futuro. *Física de la Tierra 21*, 207–218. (In Spain)

Sheffield, J. and *Wood, E.F.,* 2008. Projected changes in drought occurrence under future global warming from multi-model, multi-scenario, IPCC AR4 simulations. *Clim. Dynam. 31*, 79–105.

Simpson, I., 2011. PhD Dissertation. Precipitation variability across the UK: Observations and model simulations. Climatic Research Unit, School of Environmental Sciences, University of East Anglia, Norwich NR47TJ, UK.

Sousa P., Trigo, R.M., Aizpurua, P., Nieto, R., Gimeno, L., Garcia-Herrera, R., 2011: Trends and extremes of drought indices throughout the 20th century in the Mediterranean, NHESS, Special Issue "*Understanding dynamics and current developments of climate extremes in the Mediterranean region", 11*, 33–51.

Van Meijgaard, E., van Ulft, L.H., van de Berg, W.J., Bosvald F., van den Hurk, B., Lenderink, G., and *Siebesma A.,* 2008*:* The KNMI regional atmospheric climate model RACMO versión 2.1. *KNMI Techn. Report TR-302,* available at: www.knmi.nl/publications/fulltexts/tr302_racmo2v1.pdf

Vicente-Serrano, S.M., Beguería, S, López-Moreno, J.I., 2011: Comment on "Characteristics and trends in various forms of the Palmer Drought Severity Index (PDSI) during 1900-2008" by Aiguo Dai, *J. Geophys. Res*., *116*, D19112.